

# Acceleration and propagation of ultrahigh energy cosmic rays

**Martin Lemoine**

Institut d'Astrophysique de Paris,  
CNRS, UPMC,  
98 bis boulevard Arago, F-75014 Paris, France

E-mail: lemoine@iap.fr

**Abstract.** The origin of the highest energy cosmic rays represents one of the most conspicuous enigmas of modern astrophysics, in spite of gigantic experimental efforts in the past fifty years, and of active theoretical research. The past decade has known exciting experimental results, most particularly the detection of a cut-off at the expected position for the long sought Greisen-Zatsepin-Kuzmin suppression as well as evidence for large scale anisotropies. This paper summarizes and discusses recent achievements in this field.

## 1. Introduction

Ultrahigh energy cosmic rays are particles with energies  $\gtrsim 10^{18}$  eV that form the end of the cosmic ray spectrum. What they are and where they come from remain long-standing questions, the first detection of a  $10^{20}$  eV air shower at Volcano Ranch [1] dating back to some fifty years ago. Larger and larger detectors have been built ever since, culminating today at the scale of thousands of  $\text{km}^2$ ; and yet, this field remains data driven or actually, data starved. The extraordinarily low flux at these energies certainly implies low statistics, of the order of 1 particle per  $\text{km}^2$  and per century at  $\sim 10^{20}$  eV. As a direct consequence, the world catalogue contains only a dozen or so of events with energy  $E \gtrsim 10^{20}$  eV.

It is generally admitted that ultrahigh energy cosmic rays originate in extragalactic sources, mainly because light nuclei above  $10^{18} - 10^{19}$  eV cannot be confined in the Galactic magnetic field and because the arrival directions of ultrahigh energy cosmic rays are essentially isotropic. On top of that, only a few types of objects appear to be capable of accelerating particles to such extreme energies, and for such sources, the extragalactic flux is expected to dominate.

In such a picture, one is tempted to attribute the spectral break of the cosmic ray spectrum at  $\sim 10^{19}$  eV (the so-called ankle) to the energy at which the ultrahigh energy component emerges on top of a lower energy component. However, one cannot exclude that cosmic rays from the “second knee” at  $\sim 10^{17} - 10^{18}$  eV upwards form a single extragalactic component; in such a scenario, assuming that cosmic rays around the ankle are essentially protons, the ankle feature itself may well result from pair production of ultrahigh energy protons on the cosmic microwave background [2, 3]. Where “second knee” cosmic rays originate from and at which energy the extragalactic flux steps over the Galactic component also remain open questions; nevertheless the following discussion concentrates on extragalactic cosmic rays of energy  $\gtrsim 10^{18}$  eV. Section 2 discusses the main questions and problems, briefly summarizing at the same time the current

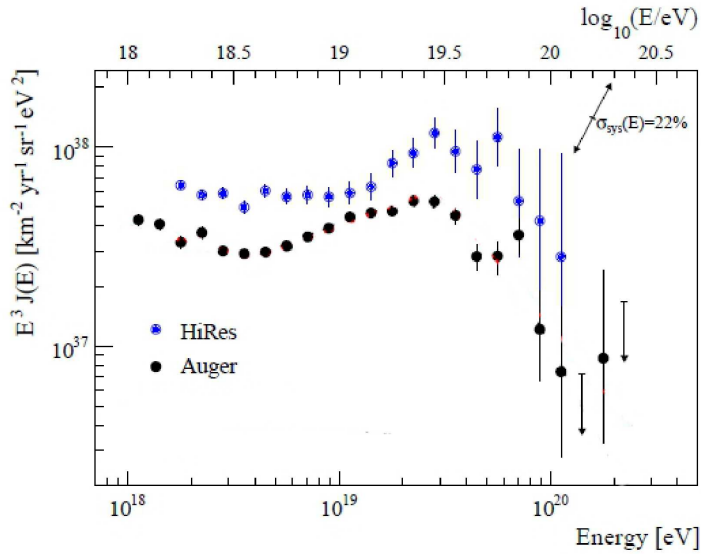


**Figure 1.** Differential spectrum of ultrahigh energy cosmic rays (multiplied by  $E^3$ ) as measured by the HiRes experiment and the Pierre Auger Observatory, revealing the cut-off at the expected location for the GZK effect. Adapted from [12].

experimental results, some of which are covered in greater detail by other papers in this volume. Section 3 focusses on the difficulties of accelerating particles to such energies, Section 4 discusses some aspects of propagation and comments on the observed anisotropies. Section 5 draws conclusions and briefly discusses some perspectives in this field.

## 2. Many questions... a few hints

The crucial questions and salient recent experimental results in this field can be categorized as follows:

### 2.1. Where does the cosmic ray spectrum stop?

One expects the spectrum to cut-off short of  $10^{20}$  eV, as the Universe becomes increasingly opaque to nuclei at these energies [4, 5] (GZK). For protons, this GZK suppression results from photo-pion interactions  $p + \gamma \rightarrow N + \pi$  (with  $N = p, n$  a nucleon) on cosmic microwave background photons, which induce energy losses  $\sim m_\pi/m_p \sim 15\%$  every interaction length  $\sim 10$  Mpc above the threshold  $\sim 6 \times 10^{19}$  eV, thereby leading to an energy loss length  $\sim 50 - 100$  Mpc. More quantitatively, 90% of protons with recorded energy  $\geq 10^{20}$  eV have travelled less than 130 Mpc, while 90% of protons with energy  $\geq 6 \times 10^{19}$  eV come from distances smaller than 200 Mpc [6].

Similar conclusions apply for nuclei with charge  $Z > 1$ , although the relevant processes are photodisintegration interactions stripping one or a few nucleons off the nucleus, through the interaction with infrared or microwave background photons. The energy loss length of iron nuclei is roughly comparable to that of protons, i.e. 90% of iron nuclei with energy above  $10^{20}$  eV originate from less than 70 Mpc, while 90% of iron nuclei with energy above  $6 \times 10^{19}$  eV originate from less than 180 Mpc [6]. The energy loss length of smaller atomic number species is smaller, all the more so as the charge becomes smaller; this effect results from the scaling of the threshold energy for photodisintegration  $\propto A$ . Helium nuclei with  $E \gtrsim 6 \times 10^{19}$  eV are thus photodisintegrated into nucleons within a few Mpc from the source, see e.g. [7, 8].

The first detection of a flux suppression above  $6 \times 10^{19}$  eV has been reported by the HiRes experiment [9]. This suppression has been confirmed by the Pierre Auger Observatory [10] and more recently by the Telescope Array experiment [11]. This feature appears clearly in the spectra measured by HiRes and by the Pierre Auger Observatory, shown in Fig. 1. Note

that the apparent discrepancy between these two spectra lies at the level of the systematic uncertainties on energy calibration, of order 20%. This discovery is in remarkable agreement with the assumption of an extragalactic ultrahigh energy cosmic ray proton spectrum. However, one must keep in mind that: (1) mixed composition spectra, with a composition for instance similar to that of Galactic cosmic rays may provide a roughly similar cut-off; (2) a maximal acceleration energy in the source at  $\sim 6 \times 10^{19}$  eV may lead to a similar propagated spectrum, even for sources located in our vicinity. Nevertheless, if one attributes this cut-off to the GZK effect, one infers that the sources of particles above  $6 \times 10^{19}$  eV are extragalactic and lie within 100Mpc. This is our cosmological backyard, so to speak.

## 2.2. What are ultrahigh energy cosmic rays?

This question is particularly crucial because, depending on the charge of the particle, one expects widely different phenomenologies. In particular, a particle of charge  $Z$  can generally be accelerated to  $Z$  times the energy of a proton but, at the same time, it is deflected by an angle  $Z$  times that of a proton in intergalactic and Galactic magnetic fields.

Unfortunately, the experimental situation is rather confuse in this respect because various experiments suggest different compositions. So far, the most reliable measurements of chemical composition have come through the determination of the maximum of shower development in the atmosphere, written  $X_{\max}$  and expressed in grammage  $\text{g}/\text{cm}^2$ , which is measured by the fluorescence telescopes that follow the longitudinal development of the air shower. The average  $\langle X_{\max} \rangle$  measured by the Fly's Eye experiment has provided indication early on that the chemical composition turns from heavy below the ankle to light above [13]. The HiRes measurements, which recover the previous Fly's Eye results where applicable, indicate a light composition up to  $\sim 10^{19.7}$  eV [14]. Recently the Pierre Auger experiment has reported measurements of  $\langle X_{\max} \rangle$  that point toward a light composition close to the ankle, which becomes increasingly heavier as the energy is increased [15]. This measurement is further supported by the trend of the fluctuations of  $X_{\max}$  from shower to shower with energy. There is still some residual discrepancy between these various indicators in the Pierre Auger data, as the fluctuations tend to suggest a heavier composition than the mean  $X_{\max}$ , but the discrepancy remains marginal at this stage. Finally, the most recent data of the Telescope Array, located in the Northern hemisphere as HiRes, also suggest a proton dominated composition up to  $10^{19.7}$  eV [16].

This situation is all the more frustrating when one realizes that the differences between the  $X_{\max}$  values of all three experiments lie within the experimental uncertainties. Thus, one cannot draw any clear information at this stage.

As emphasized below, the whole phenomenology and the interpretation of current data, as well as the prospects for the future, differ widely depending on the composition. At the highest energies, above the GZK cut-off, one would expect the composition to be dominated by iron group nuclei or by protons, since intermediate mass nuclei should have photodisintegrated on smaller distance scales, as discussed above. This statement implicitly assumes that all sources are equal: then, the flux received from sources out to distance  $d$  scales as  $d$ , so that most of the flux is received from sources located close to the horizon for particles of a given energy; as intermediate mass nuclei disappear on a length scale that is significantly smaller than the horizon of heavier nuclei or of protons, these two latter should dominate the composition at detection. One thus generally consider these two extremes, proton vs. iron group nuclei, as representative cases of differing chemical compositions. At energies below GZK, one may of course envisage that the chemical composition be more complex.

To the above two questions, one should add the following two: “what kind of source accelerates particles to such extreme energies?”, and “why do we not see the sources in the arrival directions of the highest energy cosmic rays?”. The two sections that follow are dedicated to these questions, which form the basis of most of the theoretical activity in this field.

### 3. Acceleration to ultra-high energies

Turning to theory for further clues, one should first address the problem of accelerating particles up to the extreme energies. The well-known Hillas plot [17] draws a list of possible sources of the highest energy cosmic rays by making the simple yet efficient statement that during acceleration the particles must be confined in the source on a Larmor timescale, i.e.  $r_L \leq R$ , with  $R$  the size of the source and  $r_L = \epsilon/(ZeB)$  the Larmor radius of the particle of energy  $\epsilon$  in the source magnetic field  $B$ . This criterion is well designed for non-relativistic sources but relativistic effects deserve special attention, see below. The Hillas plot provides a necessary but not sufficient condition for acceleration to a given energy. To make further progress, one needs to compare the acceleration timescale  $t_{\text{acc}}$  to all relevant timescales, e.g. [18, 19]. Then, one concludes that the leading contenders for accelerating protons to the highest energies are the most powerful radiogalaxies [20, 21], far away from the blazar zone where radiative losses prevent acceleration to ultrahigh energies, gamma-ray bursts [22, 23, 24] and young fast spinning magnetars [25, 26, 27].

#### 3.1. General considerations

One often assumes, out of simplicity, that the acceleration timescale  $t_{\text{acc}} = \mathcal{A}r_L/c$  with  $\mathcal{A} \sim 1$ . This, however is most often too optimistic. Such a statement is also frame dependent and as such it must be treated with caution. Particle acceleration requires electric fields  $E$  and in such electric fields, the equation of motion  $\mathbf{p} \cdot d\mathbf{p}/dt = q_e \mathbf{p} \cdot \mathbf{E}$  indicates that acceleration occurs (of course) as long as the particle is moving along (or against, if  $q_e < 0$ ) the electric field; then, the acceleration timescale  $t_{\text{acc}} \sim pc/(eE)$ . However  $E \leq B$  in great generality, since Ohm's law applied to the near perfectly conducting astrophysical plasmas implies  $\mathbf{E} + \mathbf{v} \times \mathbf{B}/c \simeq 0$  in a plasma moving at velocity  $\mathbf{v}$ ; thus, at the very least  $\mathcal{A} \sim c/|\mathbf{v}|$  (see also [28] for a detailed discussion). More importantly, drifting in a homogeneous coherent magnetic field does not lead to energy gain: in order to experience the voltage, particles must travel across the field lines. How such cross-field transport is realized often differentiates one acceleration mechanism from another and controls the acceleration timescale, more than often pushing  $\mathcal{A}$  to values larger or much larger than the above.

For example, non-relativistic diffusive shock acceleration leads to  $\mathcal{A} \sim \beta_{\text{sh}}^{-2} t_{\text{scatt}}/t_L \gg 1$  because the energy gain per cycle around the shock front  $\Delta E/E \sim \beta_{\text{sh}}$  but the cycle timescale  $\sim t_{\text{scatt}}/\beta_{\text{sh}}$  ( $\beta_{\text{sh}} = v_{\text{sh}}/c \ll 1$  the shock velocity in units of  $c$ ) [29]. The scattering timescale  $t_{\text{scatt}}$  is generically larger, possibly much larger than the gyration timescale  $t_L \equiv r_L/c$ , e.g. [30, 31]. In stochastic acceleration, as in the original Fermi mechanism [32], the particle diffuses in momentum space with a typical acceleration timescale corresponding to  $\mathcal{A} \sim \beta_*^{-2} t_{\text{scatt}}/t_L$ , where  $\beta_*$  represents the scattering centers velocity in units of  $c$ . In a similar process, a particle may gain energy from the electric component of turbulent waves, but  $|E_k|/|B_k| = \omega_k/(kc) \sim \beta_A$  for Alfvén waves of velocity  $\beta_A c$ . In this case therefore,  $\mathcal{A} \sim \beta_A^{-2} t_{\text{scatt}}/t_L \gg 1$  [33].

All things being equal, acceleration to extremely high rigidities thus requires relativistically moving scattering centers. If the scattering centers move as fast as the particle that is being accelerated, subtle effects come into play, see [34] for the discussion of stochastic acceleration and [35] for relativistic Fermi acceleration. It is fair to say that both schemes are not yet fully understood at the present time.

Relativistic shock acceleration deserves a special focus as it has received a great deal of attention and because it finds a natural setting in relativistic outflows. Analytical and numerical studies indicate that relativistic Fermi acceleration can be operational only at weakly magnetized shock waves, see [36, 37] and references therein. The maximal energy is limited by the fact that the particle interacts with self-generated turbulence at the microscopic scale, which is rather inefficient in terms of scattering high energy particles, meaning  $t_{\text{scatt}} \gg t_L$ . As discussed in [37, 38], a reasonable maximum energy estimate is obtained by balancing the

upstream residence time in the background unamplified magnetic field  $B_0$ , with the age  $r/c$  ( $r$  expansion radius) of the shock wave, leading to  $E_{\max} \sim Z\gamma_{\text{sh}}eB_0r$  ( $\gamma_{\text{sh}}$  shock Lorentz factor). This is  $\gamma_{\text{sh}}$  times larger than the naive Hillas estimate, but it is to be calculated in the background unamplified field, not in the self-generated turbulence. It therefore leads to a rather disappointing  $E_{\max} \sim Z \times 3 \times 10^{15} \text{ eV } \gamma_{\text{sh},2} B_{-6} r_{17}$  with  $\gamma_{\text{sh},2} \equiv \gamma_{\text{sh}}/100$ ,  $B_{-6} \equiv B/1 \mu\text{G}$ ,  $r_{17} \equiv r/10^{17} \text{ cm}$ . In short, ultra-relativistic shocks are not efficient accelerators to ultra-high energies.

Mildly relativistic shocks thus emerge as the most promising Fermi accelerators, with  $t_{\text{acc}} \sim t_{\text{scatt}}$ . Achieving  $t_{\text{acc}} \sim t_{\text{L}}$  requires the efficient generation of turbulence in the upstream with a nearly scale invariant spectrum of turbulence; whether this can be realized or not remains to be determined.

There exist of course other possible acceleration mechanisms. In magnetized rotator (pulsar) models for instance, cross-field transport to ultrahigh energies may be achieved through the ponderomotive force exerted by electromagnetic waves on the particles – provided these waves retain their coherence – or through inertia effects in the accelerating wind [26]. In rotating magnetospheres of neutrons stars and black holes, the main problem is how to tap the huge voltage – e.g.  $\Phi \sim 10^{22} V B_{15} R_6^3 P_{\text{msec}}^{-2}$  for a  $P_{\text{msec}}$  millisecond period magnetar with surface dipolar field  $B = 10^{15} B_{15} \text{ G}$  and radius  $R = 10^6 R_6 \text{ cm}$  – and how to avoid catastrophic energy losses in the rather harmful environment, see [26, 39]. Centrifugal acceleration in black hole magnetospheres operates thanks to inertia effects, which produce a drift in the direction of the convective electric field; however, the energy gain may not be sufficient to reach the ultra-high energy regime [40, 41]. Wave particle interactions have also been suggested as a mechanism to push the particles along  $\mathbf{E}$  in powerful sheared jets [28]. Shear acceleration represents an interesting variant of the Fermi process that exploits the velocity gradient of a flow to generate the motional electric fields [42], and which may lead to ultrahigh energy cosmic ray production in gamma-ray burst jets [43]. In reconnection sites, the maximal energy is limited by the extent  $l_{\text{rec}}$  of the reconnecting layer,  $E_{\max} \sim \beta_{\text{rec}} Z e B l_{\text{rec}}$  ( $\beta_{\text{rec}}$  velocity of the reconnection process in units of  $c$ ), but under certain assumptions, this might lead to  $10^{20} \text{ eV}$  particles in highly magnetized jets [44].

### 3.2. Candidate sites

Gamma-ray bursts, magnetars and powerful radio-galaxies generally rank as the top three candidates. For magnetars and/or young pulsars, see [25, 26, 27]. The expected composition is unknown but, if the particles are to be stripped off the surface of the star, a light composition appears more likely [26]. Nevertheless, assuming an ad-hoc mixed composition at the source with a hard spectrum, [27] show that the energy losses in the surrounding supernova envelope might lead to a relatively soft spectrum with a light to heavy trend with increasing energy, in satisfactory agreement with the Pierre Auger data.

Quite a few acceleration processes have been proposed in the literature to account for ultrahigh energy cosmic ray acceleration in gamma-ray bursts, e.g. acceleration in internal shocks [24], at the external shock [23], through unipolar induction [45], through stochastic interactions with internal shock fronts [46], at the reverse shock [47, 48], through stochastic acceleration behind the forward external shock [49], through shear acceleration [43], or reconnection [44]. Interestingly, if acceleration takes place in the internal shock phase, one may expect a strong neutrino signature due to proton interactions with the radiative background [50, 47]. Such a signature is now being probed by the Ice Cube experiment [51], see also [52, 53]. The possibility of detecting radiative signatures of proton acceleration to ultra-high energies has also been discussed [54]. One generally expects a light composition although heavy nuclei remain a possibility if they survive photodisintegration and spallation within the flow [55, 56]. In any case, the strongest limitation remains the energy injected in ultra-high

energy cosmic rays: gamma-ray bursts should indeed produce an isotropic equivalent  $\sim 10^{53}$  ergs in cosmic rays above  $10^{19}$  eV assuming a present day rate  $\dot{n}_{\text{GRB}} \sim 1 \text{ Gpc}^{-3} \text{ yr}^{-1}$  in order to match the observed cosmic ray flux. This is larger than the typical output energy in photons by roughly an order of magnitude, see [57, 58] for detailed estimates. Low-luminosity gamma-ray bursts, which are much more numerous, but also less powerful, represent an interesting alternative, e.g. [59, 60, 61]. Such sources can in principle push nuclei up to  $\sim Z \times 10^{19}$  eV, so that one would expect the composition to be C,N,O dominated close to the GZK cut-off.

In a way, active galactic nuclei meet opposite difficulties than gamma-ray bursts: the injection of only a moderate fraction of their bolometric luminosity would suffice to reproduce the observed cosmic ray flux above  $10^{19}$  eV [3, 62], yet they do not all offer as appetizing physical conditions with respect to particle acceleration as gamma-ray bursts. Enormous luminosities are actually required to accelerate protons to the highest energies observed, which limits the potential number of active sources in the nearby Universe (unless the highest energy cosmic rays are heavy nuclei of course). To see this, consider that acceleration takes place in an outflow, which may be moving at relativistic velocities or not, with bulk Lorentz factor  $\gamma$ , and write the acceleration timescale as before,  $t_{\text{acc}} = \mathcal{A}t_{\text{L}}$  (see also [18, 28, 63, 64, 48, 65]). In the comoving frame, the maximal energy is at least limited by the condition  $t_{\text{acc}} < t_{\text{dyn}} = R/(\gamma\beta c)$ , with  $R$  the distance to the origin the outflow, the quantity  $t_{\text{dyn}}$  defining the dynamical timescale. This inequality can be rewritten as a lower bound on the magnetic luminosity of the source, which is defined as  $L_B = R^2\Theta^2\gamma^2\beta cB^2/4$  in the laboratory or source frame:

$$L_B \geq 0.65 \times 10^{45} \Theta^2 \gamma^2 \mathcal{A}^2 \beta^3 Z^{-2} E_{20}^2 \text{ erg/s} , \quad (1)$$

with  $E_{20}$  the observed energy in units of  $10^{20}$  eV,  $\Theta$  the opening angle of the outflow and  $\beta$  the outflow velocity in units of  $c$ . Recall now that  $\mathcal{A} \gtrsim 1$  in generic acceleration processes, and often  $\mathcal{A} \gg 1$ . For protons, Eq. (1) leads to a limit that only a few sources can achieve. To be more precise, in the compilation of leptonic models by [66], only the most powerful flat spectrum radio quasars, which are thought to be the jet-on analogs of FR II radio-galaxies with relativistic jets, show a magnetic luminosity in excess of  $10^{45}$  erg/s. BL Lac objects or TeV blazars, thought to be the analogs of FR I radio-galaxies (such as Cen A) typically exhibit magnetic luminosities of the order of  $10^{44}$  erg/s or less. Recall furthermore that the above does not consider the possible radiative losses in the blazar zone, which further degrade  $E_{\text{max}}$  [18, 19, 65]. Shocks in the jets and the hot spots of the most powerful FR II radio-galaxies may nevertheless offer the requisite conditions [20, 21].

Whether one is dealing with protons or nuclei leads to very different conclusions, all the more so as  $Z \gg 1$ . For  $Z \sim 26$ , in particular, the pool of possible candidates blows up. Of course, one expects a mostly light composition on the basis of the low universal abundance of heavy nuclei; however, if protons are accelerated up to some sub-GZK energy  $E_p$ , nuclei of charge  $Z$  may well dominate beyond, up to  $ZE_p$  [8, 67]. Could the paucity of proton FR II sources in the GZK sphere (radius  $\sim 100\text{Mpc}$ ) be compensated by the acceleration of heavier nuclei in the less powerful and more numerous FR I radio-galaxies? Ptuskin and collaborators have shown that if all radio-galaxies inject a mix of light to heavy elements with a rigidity dependent maximal energy following Eq. (1),  $L_B$  being scaled to the radio luminosity, then indeed one could explain rather satisfactorily the observed spectrum [62]. However, as discussed in the following, it becomes very difficult in such scenarios to understand the observed pattern of anisotropy if one assumes that the highest energy particles are heavier than hydrogen [64].

#### 4. Transport of ultrahigh energy cosmic rays

The arrival directions are roughly isotropic in the sky and no obvious counterpart has been seen in the arrival directions of the highest energy events, in particular the world record Fly's Eye event [68] or the highest energy Auger event [69]. Departures from isotropy have been

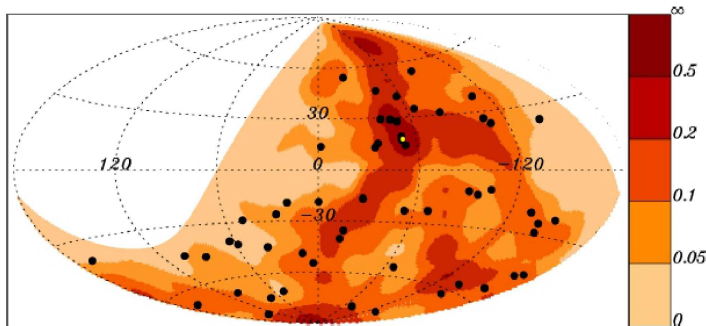


**Figure 2.** Expected flux above  $5.5 \times 10^{19}$  eV for the Pierre Auger Observatory, assuming that the sources are distributed as the galaxies of the 2MRS catalog. Black dots: Auger events; yellow dot: location of Cen A. Adapted from [74].

reported recently by the Pierre Auger Observatory through an apparent correlation of the arrival directions of cosmic rays with  $E > 6 \times 10^{19}$  eV with nearby extragalactic matter within 70 Mpc. The first data set rejected isotropy at the  $3\sigma$  level [70]. It has been shown to agree reasonably well with the distribution of large scale structure in the nearby Universe [71, 72, 69, 73]. Integrating more recent data, the evidence has slightly weakened although the signal has remained roughly at the  $3\sigma$  level. Likelihood tests of this distribution suggests a correlation with nearby large scale structure if one also allows for isotropy in a substantial fraction of arrival directions [74]. Such evidence for anisotropy has however not been recorded by the HiRes experiment in the Northern sky, which rejects correlation with large scale structure at a 95% confidence level [75]. Whether or not the discrepancy between these experiments is real remains to be proven: for one, the significance level of either claim is not so high; secondly, the energy scales of both experiment differ by some 20%, which translates in a significant difference in terms of horizon distance (hence anisotropy signal), because the horizon distance evolves rapidly with energy close to the GZK cut-off.

Most of the anisotropy pattern seen by Auger results from an apparent clustering of arrival directions around Centaurus A, see Fig. 2. Being the nearest giant radio-galaxy and a potential site of ultrahigh energy cosmic rays, Cen A has soon enough been charged of accelerating particles up to  $10^{20}$  eV. This however is too bold a step, which is not supported by theoretical and phenomenological arguments, as discussed above and further below, see also [64]. Cen A happens to lie in the direction to one the strongest concentrations of matter in the nearby Universe: the Centaurus supercluster at  $\sim 50$  Mpc and the Shapley supercluster at  $\sim 200$  Mpc; furthermore Cen A does not lie far from the zenith of the Pierre Auger Observatory. Therefore, if sources are distributed as the large scale structure, and the magnetic deflection rather weak, a cluster of events in that direction of the sky comes at no real surprise [72].

#### 4.1. Cosmic ray deflection

A cosmic ray suffers deflection in the intervening extragalactic and Galactic magnetic fields. For detailed studies on the amount of deflection for protons and nuclei in the Galactic magnetic field, see e.g. [76, 77, 78, 79]. The amount of deflection varies from direction to direction, in a way which depends sensitively on the poorly known Galactic field, but roughly, the order of magnitude is  $1^\circ$  for protons at  $10^{20}$  eV, less at high Galactic latitudes and obviously  $Z$  times more for nuclei of charge  $Z$ . At lower energies, nuclei arrival directions can suffer from lensing in the Galactic magnetic field [80].

The strength and distribution of large scale extragalactic magnetic fields are very poorly known, mostly because the origin of these magnetic fields is unknown, and because their evolution during the formation of large scale structure is far from trivial, notwithstanding all the possible sources of magnetic pollution in the late Universe. The impact of such magnetic fields on the transport of ultrahigh energy cosmic rays can be described roughly as follows.

At the highest energies, the particles only experience the rare localized regions of sufficiently intense magnetic field: the gyration radius  $r_L \simeq 10 \text{ Mpc } Z^{-1} E_{20} B_{-8}^{-1}$  is indeed much larger than the coherence length  $\lambda_B$  of intergalactic turbulence, which is bounded to  $\lesssim 100 \text{ kpc}$  [81], hence the deflection  $\delta\theta \sim l\lambda_B/r_L^2 \ll l/r_L$  in a structure of size  $l$ . Consequently, the transport of such cosmic rays can be described by a series of stochastic interactions with the peaks of the intergalactic magnetic field distribution, see [69] for a discussion. Such regions typically involve the filaments of large scale structure, which may be contaminated up to  $B_{-8} \sim 1$ , corresponding to  $\sim 10\%$  of equipartition. The direction of the cosmic ray thus follows a random walk and arrives on the detector with a typical spread of order of a few degrees for protons of  $10^{20} \text{ eV}$  on a distance scale of  $100 \text{ Mpc}$ . The dependence on the parameters characterizing the magnetic field distribution are given in Ref. [69]. The expected angular deflection is of course 26 times larger for iron nuclei of the same energy. The corresponding time delay between the arrival of a photon emitted at the same time as the cosmic ray and that of the cosmic ray is of the order of  $10^4 \text{ yrs}$ , which can explain why transient sources are not seen in the arrival direction of these highest energy particles [82].

At lower energies, the accumulated angular deflection increases, and it actually blows up rapidly below the GZK threshold, as a consequence of the rapidly increasing horizon distance, which sets the typical distance to the source, i.e. the distance from which most of the flux is collected. This geometrical effect, combined with the decreasing gyration radius, implies very large deflections, so that one should expect a roughly isotropic sky below the GZK threshold, as observed indeed.

At such energies and on such path lengths, the cosmic rays start to diffuse in the extra-galactic magnetic field. As the energy of the cosmic ray decreases further, it becomes sensitive to regions of weaker and weaker magnetic field, which have a higher filling factor in the large structure. An interesting consequence is the following: if the diffusion time scale from the closest cosmic ray source exceeds a Hubble time, the flux is suppressed. This leads to a low-energy cut-off in the extragalactic cosmic ray flux, expected around  $10^{17} - 10^{18} \text{ eV}$  for protons, i.e. in an interesting region to explain the transition between Galactic and extragalactic cosmic rays [83, 84].

#### 4.2. Anisotropy vs chemical composition

Given the numerous unknowns on the configuration of the Galactic and extragalactic magnetic fields, as well as on the charge of the particles, it is an almost impossible exercise to backtrack the position of the sources from the arrival directions in the sky with existing data. However, one may test the chemical composition on the sky by quantifying the degree of anisotropy in a particular direction as a function of energy, using the fact that sources producing heavy nuclei of charge  $Z$  at an energy  $E$  must produce a similar anisotropy pattern at energies  $E/Z$  through the proton component that is accelerated along with heavier nuclei. This test is discussed in detail in Ref. [64]. The anisotropy pattern is generally measured as an excess number of events in a region of the sky relatively to an isotropic background. Although the isotropic background "noise" increases when one goes from  $E$  to  $E/Z$ , the signal-to-noise ratio of the anisotropy pattern actually increases significantly, because the number of events in the anisotropy region also increases. This prediction does not depend on the modelling of astrophysical magnetic fields as it only relies on the property that protons of energy  $E/Z$  follow the same path in the intervening magnetic fields and produce the same angular image as heavy nuclei of charge  $Z$  and energy  $E$ , with whom they share the same magnetic rigidity.

It is useful to take as an example the observed clustering around Centaurus A, 12 events located within  $18^\circ$  out of a total of 58 events above  $55 \text{ EeV}$  for 2.7 expected for isotropic arrival directions, as of 2009. Then, assuming that the sources inject protons and iron nuclei with a chemical composition similar to that of Galactic cosmic rays (at their source), a standard  $-2$  powerlaw spectrum and maximal energy  $3 \times Z \text{ EeV}$ , so that only iron nuclei are observed at



GZK energies, one would expect an anisotropy signal many times larger (in terms of signal-to-noise ratio) at  $2 - 3\text{EeV}$  than is observed at GZK energies, see [64]. One may indeed relate the signal-to-noise ratios of the anisotropy pattern, i.e.  $\Sigma_p(> E/Z)$  for protons at  $E/Z$  and  $\Sigma_Z(> E)$  for heavy nuclei at energy  $E$  through

$$\Sigma_p(> E/Z) = \alpha_{\text{loss}} \frac{N_p}{N_Z} Z^{(1-s_{\text{obs}})/2} \Sigma_Z(> E) , \quad (2)$$

where  $N_p/N_Z$  represents the abundance ratio of proton to nuclei at the source,  $\alpha_{\text{loss}} > 1$  characterizes the influence of photodisintegration of heavy nuclei, and  $s_{\text{obs}} \simeq 2.7$  is the spectral index of the observed all particle spectrum. The above assumes for the injection spectrum a generic powerlaw function of magnetic rigidity. For a solar abundance pattern,  $Z^{(1-s_{\text{obs}})/2} N_p/N_Z$  takes values of order (100, 600, 2000) for  $Z = 8$  (CNO group),  $Z = 14$  (Si group) and  $Z = 26$  (Fe group).

This test has been applied to real data in Ref. [85] and no significant anisotropy has been observed at low energies. If the anisotropy observed at GZK energies is not a statistical accident, this result appears difficult to reconcile with a heavy composition at the highest energies. It would indeed require an extraordinarily high metallicity. On top of this, the measured all sky cosmic ray composition indicates a significant fraction of protons at low energies [14, 15]. Of course, if the clustered events at high energies are protons, the absence of anisotropies at lower energies follows naturally from magnetic smearing.

The radio-galaxy Cen A does not possess the required characteristics to accelerate protons to  $10^{20}$  eV, as discussed in Section 3.2: the jet kinetic power in Cen A  $L_{\text{jet}} \simeq 2 \times 10^{43}$  erg/s and the fit of the spectral energy distribution of the nucleus indicates  $L_B \sim 10^{42}$  ergs/sec [86]. Based on this and other arguments [31, 64], one finds that the maximal energy in Cen A does not exceed  $\sim 3 \times Z \times 10^{18}$  eV. One might argue that Cen A can accelerate heavy nuclei to GZK energies, but this would be in strong conflict with the absence of anisotropies at EeV energies. Cen A thus does not appear to be a significant source of ultrahigh energy cosmic rays. It thus seems much more conservative to interpret the clustering around Cen A as a signature of the distribution of sources in the large scale structure. Although, if gamma-ray bursts (and/or magnetars) accelerate protons to ultrahigh energies, then the last gamma-ray bursts in the host galaxy of Cen A would contribute to the flux from Cen A, due to the rescattering of the emitted particles on the giant lobes of this radio-galaxy [64], with a contribution that could account for a few events in the current Pierre Auger data set.

#### 4.3. Multi-messengers

Finally, one hope to derive indirect information of the source is to collect high energy photons or neutrinos associated to the acceleration and interaction of primary ultrahigh energy cosmic rays, either in the source or en route to the detector. One most salient result in this area is the non observation of PeV neutrinos from gamma-ray bursts by the Ice Cube experiment [51]. The current upper limit lies very close to the model prediction of Waxman & Bahcall [50, 52, 53]. If no neutrino were observed, it would not however exclude gamma-ray bursts as sources of ultrahigh energy cosmic rays, because acceleration might take place elsewhere in the source, with different secondary neutrino signatures.

An interesting result is the possible explanation of the TeV “excess” of remote blazars as the secondary photons of very high energy cosmic rays accelerated in these blazars [87] (and references therein). It is intriguing however, because this model requires a very high injected energy in cosmic rays [88], all the more so when realistic deflection in extragalactic magnetic fields is accounted for [65].

The expected flux of very high energy photons from ultrahigh energy cosmic ray sources is generally quite low, see e.g. [89, 90] for transient sources, [91, 92, 93, 94, 95] for continuous

sources. It may result from two effects: one is the production of a very high energy photon that cascades down to the GeV-TeV range through successive pair conversion and inverse Compton in the diffuse radiation fields. The observation of such photons requires very low extragalactic magnetic fields, as otherwise the electron/positron would be deflected out of the beam before transferring its energy to a background photon. Typically, this implies  $B \lesssim 10^{-13}$  G; because the cascade development is quite fast, such cascades could take place in the weakly magnetized voids of large scale structure [89, 94]. The other process is the production of an electron that radiates in synchrotron in a region of sufficient field strength, before transferring its energy to a background photon [93]. This channel is particularly interesting because it may lead to a non ambiguous signature, under the form of a degree size halo around the source in the 10 – 100 GeV range, with mild dependence on the photon energy in that range. Both channels are expected to contribute at a roughly similar level. To become detectable, a continuous source should output some  $10^{46}$  erg/s in cosmic rays at 1 Gpc, although the budget requirement becomes less at high redshift due to the evolution of diffuse backgrounds [95].

Finally, diffuse backgrounds are to be expected, among which the diffuse neutrino background at  $\sim 100$  PeV, associated to GZK interactions of cosmic ray protons. Obviously, if the composition becomes heavy close to the GZK threshold, the expected flux diminishes, down to quite pessimistic estimates [96].

## 5. Conclusions and perspectives

To summarize, the development of large scale cosmic ray detectors has led to substantially increased statistics at the highest energies and most particularly, to the discovery of the cut-off at  $6 \times 10^{19}$  eV, the expected location for the GZK cut-off beyond which the Universe becomes opaque to cosmic ray nuclei. The recent data of the Pierre Auger Observatory has also brought evidence for an increasingly heavier composition above the ankle, in apparent conflict with the chemical composition reconstructed by the HiRes and now the Telescope Array experiment. Resolving this issue becomes a priority as different chemical compositions imply different interpretations of existing data. For instance, in Sec. 3.2 it was shown that the magnetic luminosity of the source of ultrahigh energy cosmic rays must verify  $L_B \gtrsim 10^{45} Z^{-2}$  erg/s in order to accelerate particles of charge  $Z$  up to  $10^{20}$  eV. Whether one is dealing with protons or iron nuclei then leads to different conclusions. With respect to protons, only a few types of astrophysical objects seem capable of achieving acceleration to  $10^{20}$  eV, while the bound is substantially weaker for iron nuclei. Likewise, the sky map of arrival directions takes different appearances depending on the nature of the primary: for  $10^{20}$  eV protons, the expected deflection is on the order of a few degrees, while for iron nuclei, it is  $\sim 26$  times larger. In the former case, one should thus expect to see a correlation with the large scale structure at the highest energies. In the latter case of heavy nuclei primaries, the exact pattern of anisotropies, if any, is very difficult to predict with accuracy given the existing uncertainties on the configuration of the galactic magnetic field.

To constrain the chemical composition further, one may use the anisotropy pattern in the sky as a function of energy. This method has been discussed in Sec. 4.2 and applied to the apparent clustering reported by the Pierre Auger Observatory around the Cen A source. The absence of anisotropies at EeV energies then suggests that the clustered events at GZK energies are mostly protons; otherwise one would have expected to observe a much stronger anisotropy signal at EeV energies, that should be associated with the protons of a same magnetic rigidity as the hypothesized iron nuclei at GZK energies.

Regarding the perspectives in this field, one can only consider extreme cases to extrapolate the current situation, given the apparent conflict on the measurement of the chemical composition. Assume first that ultrahigh energy cosmic rays are mostly protons. Then one needs to understand of course why the Pierre Auger Observatory reports a heavier composition beyond the ankle. Only a few candidates seem capable of accelerating protons to ultrahigh energies, and the

apparent lack of counterpart in the arrival directions of the highest energy events, together with the expected small angular deflection then suggests that the source is a transient object, such as gamma-ray burst or a magnetar, camouflaged in the large scale structure. To make progress towards source identification, one needs to acquire more statistics at the highest energies to obtain a more accurate spectrum, possibly isolate clusters of events in the sky and more generally, search for the expected correlation with the large scale structure. This will be the goal of planned and future experiments such as JEM-EUSO [97] or an extension of the Pierre Auger Observatory [98]. In parallel, one should search for signatures of ultrahigh energy cosmic ray acceleration in multi-messenger signals of gamma-ray bursts and/or magnetars. As a noteworthy example, the Ice Cube experiment is now probing the PeV neutrino signal at the Waxman - Bahcall bound predicted in some scenarios of ultrahigh energy cosmic ray acceleration in gamma-ray bursts [51].

If the ultrahigh energy cosmic rays are mostly heavy nuclei, such as iron, the situation becomes unfortunately much more complex in terms of phenomenology: anisotropies should be absent or at the best weak, with a pattern that is hard to predict; theory cannot help much because the pool of source candidates is substantially larger, due to the greater facility to accelerate nuclei to  $10^{20}$  eV; finally, the possibility of detecting multi-messenger signals is considerably reduced due to the smaller Lorentz factor comparatively to protons of a same energy.

In between these two extremes lies a continuum of scenarios with mixed composition models, multi-source models... Interestingly, if protons are present up to ultrahigh energies, one recovers a situation in which only a few objects can subscribe as potential sources and in which anisotropies might be detectable, although any heavy nuclei component inputs background noise on such anisotropies. One should then focus the search on the highest rigidity particles in Nature, rather than the highest energy ones, as they must come from the most extreme sources and they likely lead to the most optimistic prospects in terms of source reconstruction.

Which scenario best describes the data is currently (and will remain for some time) the discussion of lively debates.

**Acknowledgments:** This work has been supported in part by the PEPS-PTI Program of the INP (CNRS).

## References

- [1] Linsley, J. 1963 *Phys. Rev. Lett.* 10 146
- [2] Berezhinsky V., Grigoreva, S. 1988, A bump in the ultra-high energy cosmic ray spectrum, *Astron. & Astrophys.* 199 1
- [3] Berezhinsky V., Gazizov A., Grigoreva S. 2006, On astrophysical solution to ultrahigh energy cosmic rays, *Phys. Rev. D* 74 043005
- [4] Greisen, K. 1966 *Phys. Rev. Lett.* 16 748
- [5] Zatsepin G. T., Kuzmin V. A. 1966 *Sov. J. Exp. Theor. Phys. Lett.* 4 78
- [6] Harari D., Mollerach S., Roulet E. 2006 *J. Cosm. Astropart. Phys.* 11 012
- [7] Bertone G., Isola C., Lemoine M., Sigl G. 2002 *Phys. Rev. D* 66 103003
- [8] Allard D., Busca N. G., Decerprit G., Olinto A. V., Parizot E. 2008 *J. Cosm. Astropart. Phys.* 10 033
- [9] Abbasi R. U. et al. (The HiRes Collaboration) 2008 *Phys. Rev. Lett.* 100 101101
- [10] Abraham J. et al. (The Pierre Auger Collaboration) 2008 *Phys. Rev. Lett.* 101 061101
- [11] Abu-Zayyad T. et al. (The Telescope Array Collaboration) 2012 arXiv:1205.5067
- [12] Dawson B. 2011 *AIPC Conf. Proc.* 1367 11
- [13] Bird D. J. et al. (The Fly's Eye Collaboration) 1993 *Phys. Rev. Lett.* 71 3401
- [14] Abbasi R. U. et al. (The HiRes Collaboration) 2010 *Phys. Rev. Lett.* 104 161101
- [15] Abraham, J., Abreu, P., Aglietta, M. et al. (The Pierre Auger Collaboration) *Phys. Rev. Lett.*, 104, 091101, 2010.
- [16] Sagawa H. 2011 *AIPC Conf. Proc.* 1367 17
- [17] Hillas A. M. 1984 *Ann. Rev. Astron. Astrophys.* 22 425
- [18] Norman C. A., Melrose D. B., Achterberg A. 1995 *Astrophys. J.* 454 60
- [19] Henri G., Pelletier G., Petrucci P.-O., Renaud N. 1999 *Astropart. Phys.* 11 347

- [20] Takahara F. 1990 *Prog. Theor Phys.* 83 1071
- [21] Rachen J. P., Biermann P. L., 1993 *Astron. Astrophys.* 272 161
- [22] Milgrom M., Usov V. 1995 *Astrophys. J. Lett.* 449 37
- [23] Vietri M. 1995 *Astrophys. J.* 453 883
- [24] Waxman E. 1995 *Phys. Rev. Lett.* 75 386
- [25] Blasi P., Epstein R. L., Olinto A. V. 2000 *Astrophys. J.* 533 L123
- [26] Arons J. 2003 *Astrophys. J.* 589 871
- [27] Fang K., Kotera K., Olinto A. V. 2012 *Astrophys. J.* 750 118
- [28] Lyutikov M., Ouyed R. 2007 *Astropart. Phys.* 27 473
- [29] Blandford R., Eichler D. 1987 *Phys. Rep.* 154 1
- [30] Pelletier G. 2001 *Lect. Notes in Phys.* 576 58
- [31] Casse F., Lemoine M., Pelletier G. 2002 *Phys. Rev. D* 65 023002
- [32] Fermi E. 1949 *Phys. Rev.* 75 1169
- [33] O'Sullivan S., Reville B., Taylor A. M. 2009 *Month. Not. Roy. Astron. Soc.* 400 248
- [34] Pelletier G. 1999 *Astron. Astrophys.* 350 705
- [35] Gallant Y., Achterberg A. 1999 *Month. Not. Roy. Astron. Soc.* 305 L6
- [36] Lemoine M., Pelletier G. 2010 *Month. Not. Roy. Astron. Soc.* 402 321
- [37] Lemoine M., Pelletier G. 2012 *AIPC Conf. Proc.* 1439 194
- [38] Plotnikov I., Pelletier G., Lemoine M. 2012 arXiv:1206.6634
- [39] Berezhinsky V. S., Bulanov S. V., Dogiel V. A., Ptuskin V. S. 1990 *Astrophysics of cosmic rays* (Amsterdam: North-Holland) ed. Ginzburg V. L.
- [40] Rieger F. M., Aharonian F. A. 2008 *Astron. Astrophys.* 479 L5
- [41] Istomin Y. N., Sol H. 2009 *Astrophys. Sp. Sc.* 321 57
- [42] Rieger F., Bosch-Ramon V., Duffy P. 2007 *Astrophys. Sp. Sc.* 309 119
- [43] Rieger F., Duffy P. 2005 *Astrophys. J.* 632 L21
- [44] Giannios D. 2010 *Month. Not. Roy. Astron. Soc.* 408 L46
- [45] Milgrom M., Usov V. 1996 *Astropart. Phys.* 4 365
- [46] Gialis D., Pelletier G. 2004 *Astron. Astrophys.* 425 395
- [47] Waxman E. 2001 *Lect. Notes in Phys.* 576 122
- [48] Dermer C. D., Razzaque S. 2010, *Astrophys. J.* 724 1366
- [49] Dermer C. D., Humi M. 2001 *Astrophys. J.* 556 479
- [50] Waxman E., Bahcall J. 1997 *Phys. Rev. Lett.* 78 2292
- [51] Abbasi R. et al. (The Ice Cube Collaboration) 2012 *Nature* 484 351
- [52] Hümmel S., Baerwald P., Winter W. 2012 *Phys. Rev. Lett.* 108 1101
- [53] He H.-N., Liu R.-Y., Wang X.-Y., Nagataki S., Murase K., Dai Z.-G. 2012 *Astrophys. J.* 752 29
- [54] Asano K., Inoue S., Mészáros P. 2009 *Astrophys. J.* 699 953
- [55] Lemoine M. 2002 *Astron. Astrophys.* 390 L31
- [56] Wang X.-Y., Razzaque S., Mészáros P. 2008 *Astrophys. J.* 677 432
- [57] Katz B., Budnik R., Waxman E. 2009 *J. Cosm. Astropart. Phys.* 03 020
- [58] Eichler D., Guetta D., Pohl M. 2010 *Astrophys. J.* 722 543
- [59] Wang X.-Y., Razzaque S., Mészáros P., Dai Z.-G. 2007 *Phys. Rev. D* 76 083009
- [60] Liu R.-Y., Wang X.-Y., Dai Z.-G. 2011 *Month. Not. Roy. Astron. Soc.* 418 1382
- [61] Liu R.-Y., Wang X.-Y. 2012 *Astrophys. J.* 746 40
- [62] Ptuskin V. S., Rogovaya S. I., Zirakashvili V. N. 2011 arXiv:1105.4491
- [63] Waxman E. 2005 *Physica Scripta Volume T* 121 147
- [64] Lemoine M., Waxman E. 2009 *J. Cosm. Astropart. Phys.* 11 009
- [65] Murase K., Dermer C. D., Takami H., Migliori G. 2012 *Astrophys. J.* 749 63
- [66] Celotti A., Ghisellini G. 2008 *Month. Not. Roy. Astron. Soc.* 385 283
- [67] Aloisio R., Berezhinsky V., Gazizov A. 2012 *J. Phys.: Conf. Ser.* 337 012042
- [68] Elbert J. W., Sommers P. 1995 *Astrophys. J.* 441 151
- [69] Kotera K., Lemoine M. 2008 *Phys. Rev. D* 77 123003
- [70] Abraham J. et al. (The Pierre Auger Collaboration) 2008 *Astropart. Phys.* 29 188
- [71] Ghisellini G., Ghirlanda G., Tavecchio F., Fraternali F., Pareschi G. 2008 *Month. Not. Roy. Astron. Soc.* 390 L88
- [72] Kashti T., Waxman E. 2008 *J. Cosm. Astropart. Phys.* 5 006
- [73] Koers H. B. J., Tinyakov P. 2009 *J. Cosm. Astropart. Phys.* 04 003
- [74] Abreu et al. (The Pierre Auger Collaboration) 2010 *Astropart. Phys.* 34 314
- [75] Abbasi R. U. et al. (The HiRes Collaboration) 2010 *Astrophys. J. Lett.* 713 64
- [76] Alvarez-Muñiz J., Stanev T. 2006 *J. Phys.: Conf. S.* 47 126

- [77] Takami H., Sato K. 2008 *Astrophys. J.* 681 1279
- [78] Giacinti G., Kachlriess M., Semikoz D. V., Sigl G. 2010 *J. Cosm. Astropart. Phys.* 08 036
- [79] Takami H., Inoue S., Yamamoto T. 2012 *Astropart. Phys.* 35 767
- [80] Harari D., Mollerach S., Roulet E. 2002 *J. High E. Phys.* 03 045
- [81] Waxman E., Bahcall J. 1999 *Phys. Rev. D* 59 3002
- [82] Waxman E., Miralda-Escudé J. 1996 *Astrophys. J.* 472 L89
- [83] Lemoine M. 2005 *Phys. Rev. D* 71 083007
- [84] Aloisio R., Berezhinsky V. S. 2005 *Astrophys. J.* 625 249
- [85] Abreu, P. et al. (The Pierre Auger Collaboration) 2011, *J. Cosm. Astropart. Phys.* 06 022
- [86] Chiaberge M., Capetti A., Celotti A. 2001 *Month. Not. Roy. Astron. Soc.* 324 L33
- [87] Essey W., Kusenko A. 2010 *Astropart. Phys.* 33 81
- [88] Razzaque S., Dermer C. D., Finke J. D. 2012 *Astrophys. J.* 745 196
- [89] Waxman E., Coppi P. 1996 *Astrophys. J.* 464 L75
- [90] Murase K. 2012 *Astrophys. J.* 745 L16
- [91] Aharonian F. 2002 *Month. Not. Roy. Astron. Soc.* 332 215
- [92] Ferrigno C., Blasi P., de Marco D. 2004 *Nuc. Phys. B Proc. Supp.* 136 191
- [93] Gabici S., Aharonian F. 2005 *Phys. Rev. Lett.* 95 251102
- [94] Kotera K., Allard D., Lemoine M. 2011 *Astron. Astrophys.* 527 54
- [95] Prosekin A. Yu., Kelner S. R., Aharonian F. A. 2011, *Astron. Astrophys.* 536 30
- [96] Kotera K., Allard D., Olinto A. V. 2010 *J. Cosm. Astropart. Phys.* 10 013
- [97] Ebisuzaki T. et al. (The JEM-EUSO Collaboration) 2011 *AIP Conf. Proc.* 1367 120
- [98] Abraham, J. et al. (The Pierre Auger Collaboration) 2009 *31<sup>st</sup> ICRC* arXiv:0906.2354